Journal of Computations & Modelling, vol.4, no.2, 2014, 127-150
ISSN: 1792-7625 (print), 1792-8850 (online)
Scienpress Ltd, 2014

Visualization Technique for Real-Time Detecting the Characteristic Quantities Critical Values During Electrical Transient Episodes

Lucian Lupşa-Tătaru[1]

Abstract

The traditional approach to detecting the critical values of the characteristic quantities that comprehensively describe an electrical transient scenario involves generating huge files that contain the data received at all steps during numerical integration, and the application of an optimization method to approximate the critical values. Having in view that the straight numerical depicting of an electrical transient, performed by recording all the data during numerical integration i.e. without highlighting the areas of interest that encompass the characteristic quantities critical values, is very time consuming and unsuitable for real-time evaluation, distinct from the time-domain assessment, the present investigation advances a visualization technique for detecting the critical values of the characteristic quantities that describe an electrical transient episode. The suggested technique requires the employment of a coordinate system in two dimensions with the abscissa represented by a certain characteristic quantity value and the ordinate

[1] Department of Electrical Engineering and Applied Physics, Faculty of Electrical Engineering and Computer Science, Transilvania University, Bd. Eroilor No. 29, Braşov, Romania. E-mail: lupsa@programmer.net

Article Info: *Received* : March 27, 2014. *Revised* : May 2, 2014.
Published online : May 31, 2014.

represented by the corresponding time-related derivative of the characteristic quantity. By means of various diagrams of practical significance, it will be shown that the employment of the adopted coordinate system, accompanied by setting viewports through an appropriate restriction of the ordinate interval, makes it possible to detect in real-time the characteristic quantities critical values.

Mathematics Subject Classification: 37J35; 65L06; 65Y20; 68U20; 93A30
Keywords: Electrical transient, Critical values detection, Data visualization, Ordinary differential equations, Software environment

1 Introduction

At present, various software environments designed for the electrical transients evaluation are extensively employed to solve in off-line mode different scenarios that highlight the dynamic performances of electrical systems. The characteristic quantities, which comprehensively describe a particular transient episode, are traditionally represented in the time-domain, over the entire selected interval. It has to be emphasized that the straight accurate solving of a transient scenario, which is performed by recording all the data during numerical integration i.e. without highlighting the areas of interest that encompass the critical values, is convenient but very time consuming and unsuitable for online dynamic security assessment since the amount of recorded data is not being optimized [1].

It is widely accepted that knowing merely the critical values of the characteristic quantities describing different transient scenarios is sufficient to assess the dynamic performance of the electrical system under evaluation. Thus, the approach to real-time assessment of the electrical transient episodes [2-4] is frequently directed toward emphasizing only the significant data i.e. data that best approximate the characteristic quantities critical values. In this context, the approach put forward in [5] aims at an assessment in the time-domain but with the avoiding of recording all the data received during numerical integration of the system of ordinary differential equations that describes a particular transient scenario. In this manner, only restricted areas of interest, encompassing the stationary points and the corresponding critical values, are highlighted in order to depict the topology of the characteristic quantities evolution curves.

Distinct from the time-domain analysis, the present investigation aims at detecting the critical values (relative extrema) of the characteristic quantities, which comprehensively describe an electrical transient episode, in real-time i.e. during the numerical integration process by introducing a coordinate system in two dimensions with the abscissa represented by the characteristic quantity value and the ordinate represented by the characteristic quantity time-related derivative. We have to emphasize that a characteristic quantity here does not designate necessarily a state variable, which has to be updated at each step of numerical integration, but more generally, a characteristic quantity can be here provided by any closed-form expression in terms of state variables.

It is well-known that a phase plane that has the abscissa represented by the position (current, voltage, flux linkage) and the ordinate represented by the velocity i.e. the position time-related derivative [6] is usually adopted as a starting point in order to eventually plot the phase line corresponding to an autonomous ordinary differential equation:

$$\frac{dy}{dt} = g\left(y\right).$$

In this case, the phase line is used to assess the transient performance of the electrical system under study, having in view that there is a single state variable and that the critical values (equilibria) are the solutions of $g\left(y\right) = 0$.

The evaluation suitable for systems described by an autonomous ordinary differential equation cannot be extended to electrical systems described by means of multiple state variables i.e. by means of systems of ordinary differential equations, given that the stationary points are not the same for all state variables. However, by means of various diagrams, it will be shown that the employment of the adopted Cartesian coordinate system for any characteristic quantity makes it possible to detect in real-time, i.e. during the numerical integration process, the critical values occurring in the course of the electrical transient episode. The suggested visualization technique involves setting of viewports by restricting the domain of the characteristic quantities time-related derivatives.

To present the visualization technique, we will consider the state-space model and the numerical integration method put forward in [5], materialised there in the employment of a high-order Adams-Bashforth method with the purpose of real-time localizing the critical values of a synchronous generator phase current, occurring at sudden three-phase short circuit fault. Hence, having in view that the adopted system model, state-space model and numerical integration method are presented in detail in [5], the system under evaluation will now be depicted in a very compact manner. However, the initial condition used to generate the particular transient short circuit scenario will be emphasized.

2 The System Model and the State-Space Model

The orthogonal axis mathematical model of a salient-pole synchronous generator endowed with damping cage is considered [7-9]. By treating this intricate case, the reader will receive more insight upon the suggested technique, having in view that, in this situation, the characteristic quantities, which comprehensively describe a transient scenario, are not identical to the set of state variables, selected in the orthogonal *d-q* reference frame. As it is well-established, the set of differential equations i.e. the set of voltage equations of the generalized *d-q* axis mathematical model of synchronous generators emphasizes the time-related derivatives of the *d*-*q* axis winding flux linkages:

$$\frac{d\,\psi_d\left(i_d\,,i_f\,,i_D\right)}{dt}=\omega_r\;\psi_q\left(i_q\,,i_Q\right)-R\,i_d-u_d\;, \tag{1}$$

$$\frac{d\,\psi_q\left(i_q\,,i_Q\right)}{dt}=-\,\omega_r\;\psi_d\left(i_d\,,i_f\,,i_D\right)-R\,i_q-u_q\;, \tag{2}$$

$$\frac{d\,\psi_f\left(i_d\,,i_f\,,i_D\right)}{dt}=-R_f\,i_f+u_f\;, \tag{3}$$

$$\frac{d\,\psi_D\left(i_d\,,i_f\,,i_D\right)}{dt}=-R_D\,i_D\;, \tag{4}$$

$$\frac{d\,\psi_Q\left(i_q\,,i_Q\right)}{dt}=-R_Q\,i_Q \tag{5}$$

whilst the set of algebraic correlations i.e. the well-established set of flux equations yields each winding flux linkage in terms of the *d*-*q* axis winding currents:

$$\begin{aligned}\psi_d\left(i_d\,,i_f\,,i_D\right)&=L_d\,i_d+L_{md}\cdot\left(i_f+i_D\right);\\ L_d&=L_\sigma+L_{md}\;,\end{aligned} \tag{6}$$

$$\begin{aligned}\psi_q\left(i_q\,,i_Q\right)&=L_q\,i_q+L_{mq}\,i_Q\;;\\ L_q&=L_\sigma+L_{mq}\;,\end{aligned} \tag{7}$$

$$\begin{aligned}\psi_f\left(i_d\,,i_f\,,i_D\right)&=L_f\,i_f+L_{md}\cdot\left(i_d+i_D\right);\\ L_f&=L_{f\sigma}+L_{md}\;,\end{aligned} \tag{8}$$

$$\begin{aligned}\psi_D\left(i_d\,,i_f\,,i_D\right)&=L_D\,i_D+L_{md}\cdot\left(i_d+i_f\right);\\ L_D&=L_{D\sigma}+L_{md}\;,\end{aligned} \tag{9}$$

$$\begin{aligned}\psi_Q\left(i_q\,,i_Q\right)&=L_Q\,i_Q+L_{mq}\,i_q\;;\\ L_Q&=L_{Q\sigma}+L_{mq}\;.\end{aligned} \tag{10}$$

The symbols and the subscripts interfering in (1)-(10) are as follows: u - voltage; i - current; ψ - flux linkage; t - time variable (instant); ω_r - rotor angular velocity; R - resistance; L - inductance; d - denotes *d*-axis (“direct” axis) components; q - denotes *q*-axis (“quadrature” axis) components; f - denotes variables and parameters associated with field winding; D, Q - denote variables and parameters associated with *d*-*q* axis damper circuits; σ - denotes leakage inductances; *m* - denotes the *d*-*q* axis magnetizing inductances.

Correlations (6)-(10) allow us to select the set of state variables in different variants (*d*-*q* axis currents and/or *d*-*q* axis flux linkages). Assuming that the generator parameters are of constant value and having in view that the transient currents are of primary practical interest, we will preserve all *d*-*q* axis winding currents as state variables.

Hence, since the *d*-*q* axis currents stand here for state variables, we will straightforwardly employ the state-space model in the form developed in [5], where it had been used to carry out time-domain simulations with the purpose of highlighting the areas of interest, encompassing the stationary points and the critical values of generator stator phase current. Thus, the state-space model is [5]:

$$\frac{d}{dt}\mathbf{I} = \mathbf{C} \times \mathbf{I} + \mathbf{D} \times \mathbf{U} \tag{11}$$

where

$$\mathbf{I} = \begin{bmatrix} i_d & i_q & i_f & i_D & i_Q \end{bmatrix}^T,$$

$$\mathbf{U} = \begin{bmatrix} u_d & u_q & u_f \end{bmatrix}^T$$

are the state currents vector and the voltages vector, while **C** and **D** are the matrices of currents and voltages coefficients.

The boundary (restrictive) condition corresponding to sudden three-phase short circuit fault [9-11], which is selected here as the transient scenario, is

$$u_A(t) \equiv u_B(t) \equiv u_C(t) \equiv 0.$$

Applying the direct Park-Gorev transformation [7, 8], which performs the mapping of stator winding variables to the *d*-*q* axis reference frame, we immediately get the stator *d*-*q* axis voltages during the sudden three-phase short circuit:

$$u_d = \frac{2}{3}\left[u_A \cos\gamma + u_B \cos\left(\gamma + \frac{2\pi}{3}\right) + u_C \cos\left(\gamma + \frac{4\pi}{3}\right)\right] \equiv 0, \tag{12}$$

$$u_q = \frac{2}{3}\left[u_A \sin\gamma + u_B \sin\left(\gamma + \frac{2\pi}{3}\right) + u_C \sin\left(\gamma + \frac{4\pi}{3}\right)\right] \equiv 0\,. \qquad (13)$$

The converse Park-Gorev transformation [7, 8] is required for computing the values of stator phase currents having at hand the stator *d-q* axis currents, which are state variables:

$$i_A = i_d \cos\gamma + i_q \sin\gamma\,, \qquad (14)$$

$$i_B = i_d \cos\left(\gamma + \frac{2\pi}{3}\right) + i_q \sin\left(\gamma + \frac{2\pi}{3}\right), \qquad (15)$$

$$i_C = i_d \cos\left(\gamma + \frac{4\pi}{3}\right) + i_q \sin\left(\gamma + \frac{4\pi}{3}\right) \qquad (16)$$

where

$$\gamma(t) = \gamma_0 - \omega_r\, t \qquad (17)$$

is the rotor lag angle given as function of time variable only, having in view that rotor angular velocity ω_r is assumed constant and equal to synchronous velocity ω_n while γ_0, as the initial value of rotor lag angle, is provided at the beginning of the numerical integration process. In order to set the initial value problem, state-space model (11) is coupled with the initial condition of no-load operation:

$$(i_d)_0 = 0\,,\ (i_q)_0 = 0\,,\ (i_f)_0 = I_{fn}\,,\ (i_D)_0 = 0\,,\ (i_Q)_0 = 0 \qquad (18)$$

wherein the initial value of field current (subscript “*f* ”) equals the rated value.

Since the key characteristic quantities are the stator phase currents, in order to emphasize the benefits of the visualization technique proposed in this paper, we will proceed to plot diagrams in the Cartesian coordinate system with the abscissa represented by the stator phase *A* current and the ordinate represented by the stator phase *A* current derivative, for different initial values of rotor lag angle i.e. for different values of γ_0 in (17). Out of (14) we receive the stator phase *A* current derivative in terms of the stator *d-q* axis currents, which are state variables, and their time-related derivatives that are by default evaluated at each step of numerical integration:

$$\frac{di_A}{dt} = \left(\frac{di_d}{dt} - \omega_r\, i_q\right)\cos\gamma + \left(\frac{di_q}{dt} + \omega_r\, i_d\right)\sin\gamma\,. \tag{19}$$

3 Data Visualization

3.1 The Traditional Approach

Figure 1 illustrates the time-related evolution curves of stator phase *A* current, occurring at the sudden three-phase short circuit of a salient-pole synchronous generator with the following dimensionless (per unit) parameters [9]:

- resistances: $\begin{cases} R = 0.0256 \text{ p.u.}, \\ R_f = 0.0032 \text{ p.u.},\ R_D = 0.088 \text{ p.u.},\ R_Q = 0.036 \text{ p.u.} \end{cases}$

- leakage inductances: $\begin{cases} L_\sigma = 0.088 \text{ p.u.}, \\ L_{f\sigma} = 0.258 \text{ p.u.},\ L_{D\sigma} = 0.33 \text{ p.u.},\ L_{Q\sigma} = 0.066 \text{ p.u.} \end{cases}$

- the *d*-*q* axis magnetizing inductances: $L_{md} = 1.31$ p.u., $L_{mq} = 0.705$ p.u.

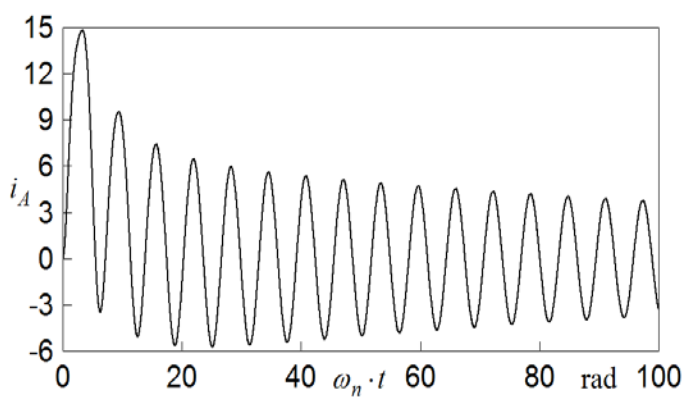

Figure 1(a): Evolution curve of stator phase current (14) for $\gamma_0 = 0$

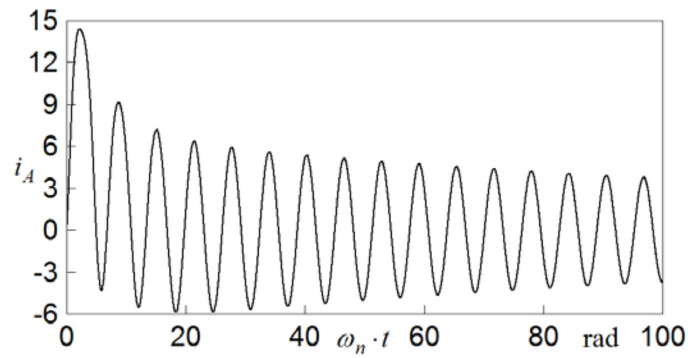

Figure 1(b): Evolution curve of stator phase current (14) for $\gamma_0 = -\pi/6$

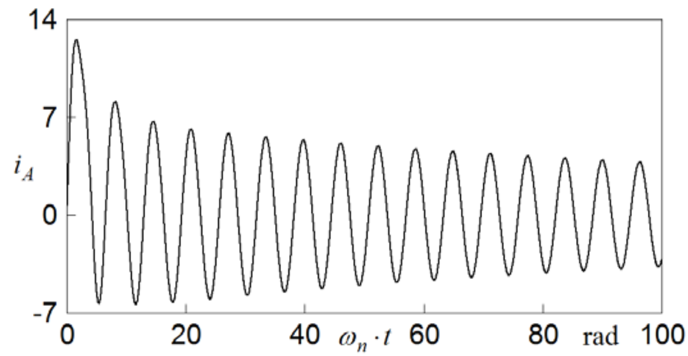

Figure 1(c): Evolution curve of stator phase current (14) for $\gamma_0 = -\pi/3$

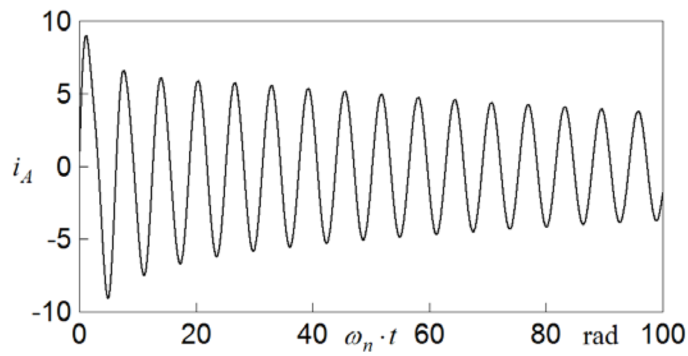

Figure 1(d): Evolution curve of stator phase current (14) for $\gamma_0 = -\pi/2$

Figure 1: Evolution curves of stator phase current for different circumstances: (a) $\gamma_0 = 0$; (b) $\gamma_0 = -\pi/6$; (c) $\gamma_0 = -\pi/3$; (d) $\gamma_0 = -\pi/2$

The curves of Figure 1 are plotted for the initial values of rotor lag angle $\gamma_0 \in \{0, -\pi/6, -\pi/3, -\pi/2\}$. The numerical integration has been performed by employing the Adams-Bashforth method derived in [5]. The curves in Figure 1(a) till Figure 1(d) plainly illustrate the traditional manner of depicting the transient performance of an electrical system. More precisely, the highlighting in real-time of the areas of interest, encompassing the stationary points and the critical values that are of utmost practical significance, is not a purpose of the traditional approach and, hence, in order to approximate the critical values, the system analyst has to wait for the data of all steps of numerical integration to be recorded within a huge file and, later on, to apply an optimization method.

3.2 The Proposed Technique

To make the data more useful with a view to critical values detection, we proceed to introduce a new coordinate system. The abscissa will be represented by the characteristic quantity and the ordinate will be represented by the characteristic quantity derivative. Such kind of representation is usually performed to merely evaluate the dynamic behaviour of a system described by an autonomous ordinary differential equation. The curves plotted in Figure 2 represent the set of points determined by the stator phase A current and its time-related derivative i.e. $\left(i_A,\ di_A/dt\right)$ for the initial values of rotor lag angle $\gamma_0 \in \{0, -\pi/6, -\pi/3, -\pi/2\}$.

We recall that the initial value of rotor lag angle interferes in (17) and, implicitly, decides the evolution of stator phase A current (14) and of its corresponding time-related derivative (19). The set of points $\left(i_A,\ di_A/dt\right)$ has been determined and recorded in real-time i.e. simultaneous with the numerical integration of system (11). The recording in real-time of stator phase A current derivative (19) has been manageable due to the fact that the information needed by the Adams-Bashforth method in order to update the state currents incorporates the state currents time-related derivatives at some previous steps of integration [5, 12, 13] and because, in contrast to most of software environments designed for electrical transients assessment, the recent values of state currents derivatives have not been discharged immediately after the state currents updating.

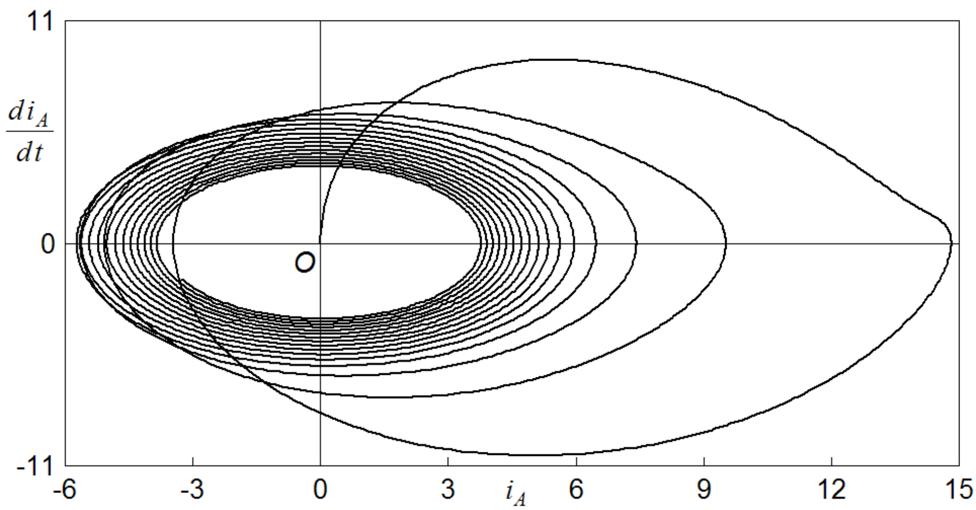

Figure 2(a): Phase trajectory for $\gamma_0 = 0$ in (17)

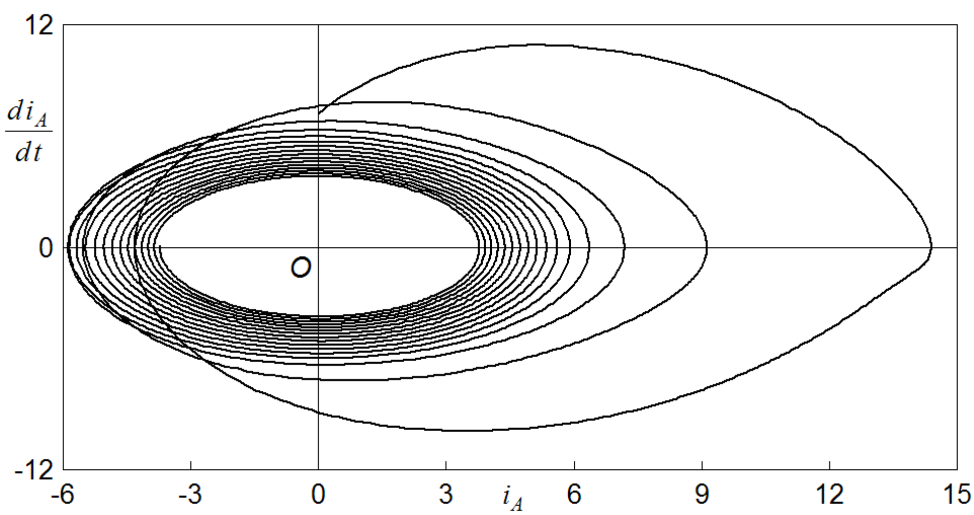

Figure 2(b): Phase trajectory for $\gamma_0 = -\pi/6$ in (17)

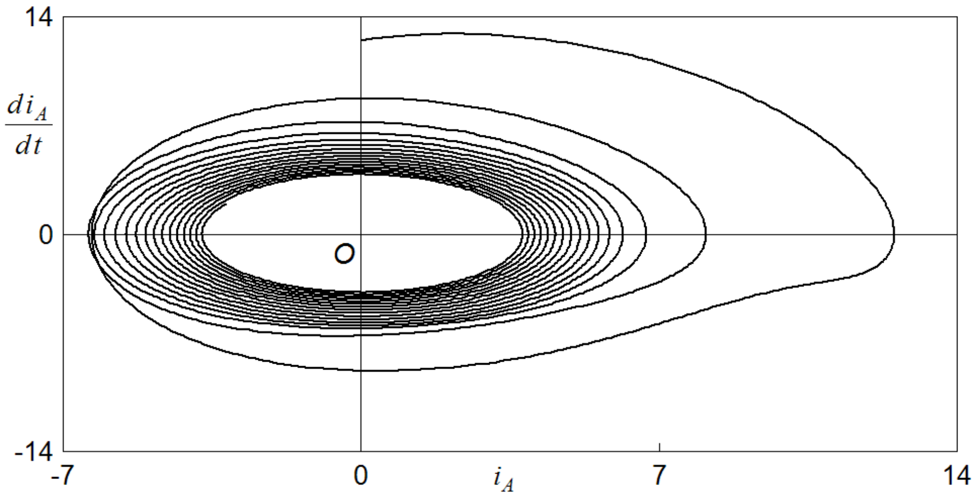

Figure 2(c): Phase trajectory for $\gamma_0 = -\pi/3$ in (17)

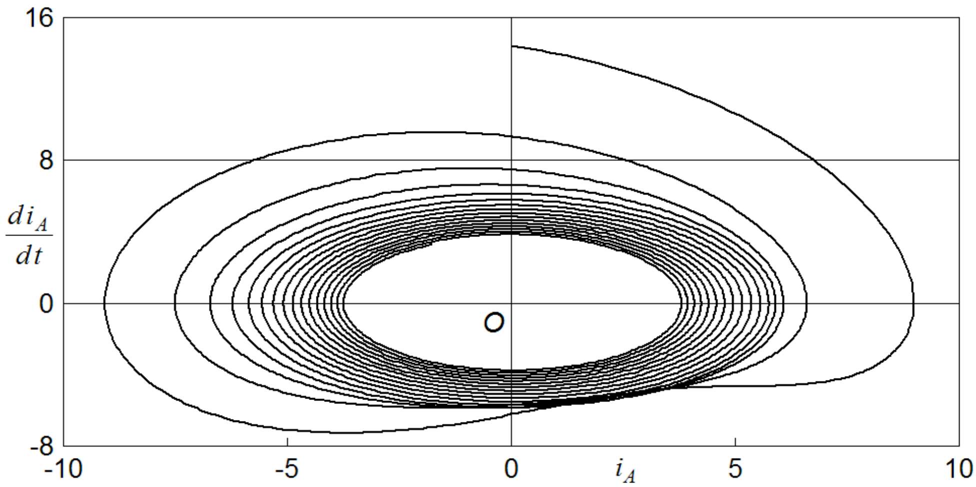

Figure 2(d): Phase trajectory for $\gamma_0 = -\pi/2$ in (17)

Figure 2: Trajectories plotted by employing the Cartesian coordinate system with stator phase *A* current and stator phase *A* current time-related derivative as coordinates, for different circumstances:
(a) $\gamma_0 = 0$; (b) $\gamma_0 = -\pi/6$; (c) $\gamma_0 = -\pi/3$; (d) $\gamma_0 = -\pi/2$

Notice that all variables are provided in the per unit (p.u.) dimensionless system. It has to be emphasized that although merely the critical values are of significant practical interest, all curves in Figure 1 and Figure 2 are the result of accessing huge files that contain the data recorded at all steps of numerical integration. In the time-domain, with the purpose of highlighting the areas of interest, encompassing the critical values, and in order to improve the computational capabilities, in [5] we have introduced a procedure that allows the recording of only significant data during the numerical integration process. Relative to the plots in Figure 2, achieved by adopting the new coordinate system, it comes to be clear that the critical values are to be found at the intersection of the curves with the axis of abscissae i.e. the axis of stator phase *A* current values. Therefore, in the adopted coordinate system, to localize the areas of interest, encompassing the critical values, we have to proceed in a manner similar to that in [5] i.e. one has to restrict the domain of the values of characteristic quantities time-related derivatives. To improve legibility in presentation and to offer the reader more understanding upon the suggested visualization technique, in Figure 3 up to Figure 6 the relative minima and the relative maxima are encompassed in distinct diagrams, employing the adopted Cartesian coordinate system. Such kind of data visualization comes to be useful when there is a large difference between the minimum value of the set of relative maxima and the maximum value of the set of relative minima.

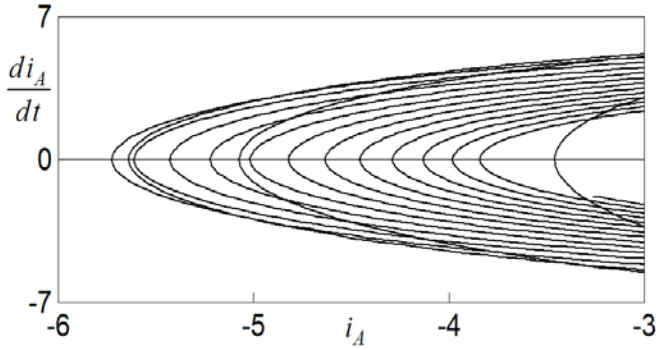

Figure 3(a): Diagram encompassing the stator phase current relative minima

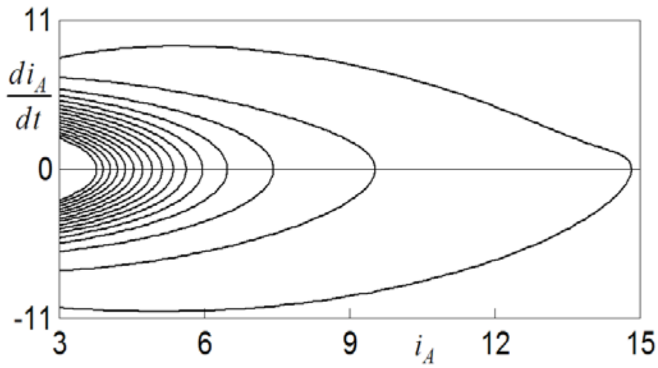

Figure 3(b): Diagram encompassing the stator phase current relative maxima

Figure 3: Pair of diagrams encompassing the relative minima and the relative maxima of stator phase current (14), respectively, for $\gamma_0 = 0$ in (17)

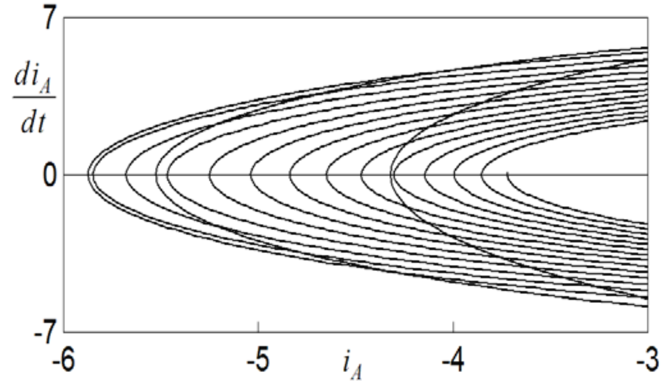

Figure 4(a): Diagram encompassing the stator phase current relative minima

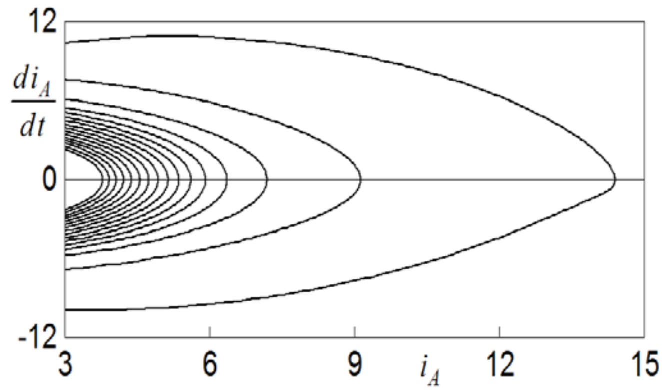

Figure 4(b): Diagram encompassing the stator phase current relative maxima

Figure 4: Pair of diagrams encompassing the relative minima and the relative maxima of stator phase current (14), respectively, for $\gamma_0 = -\pi/6$ in (17)

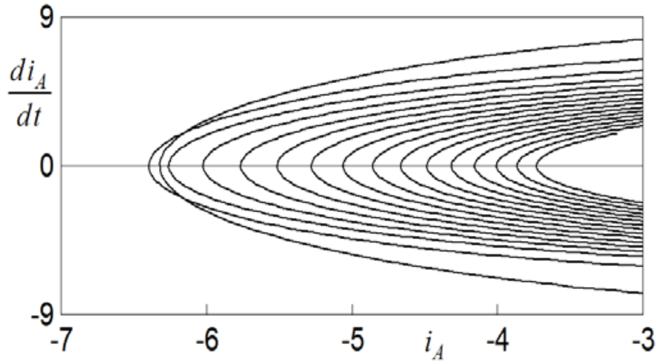

Figure 5(a): Diagram encompassing the stator phase current relative minima

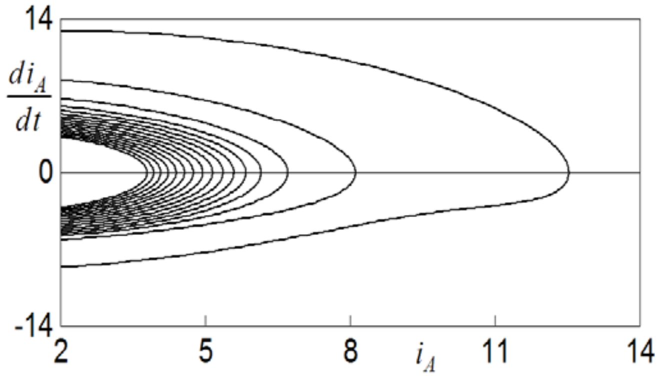

Figure 5(b): Diagram encompassing the stator phase current relative maxima

Figure 5: Pair of diagrams encompassing the relative minima and the relative maxima of stator phase current (14), respectively, for $\gamma_0 = -\pi/3$ in (17)

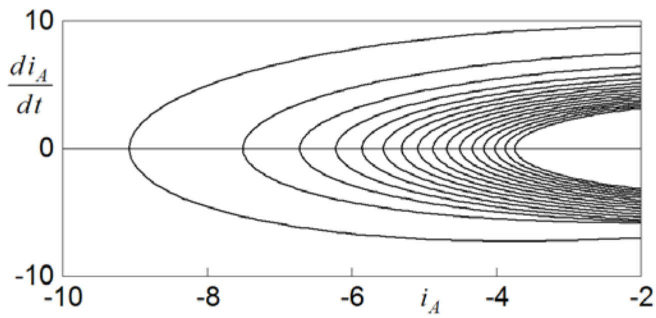

Figure 6(a): Diagram encompassing the stator phase current relative minima

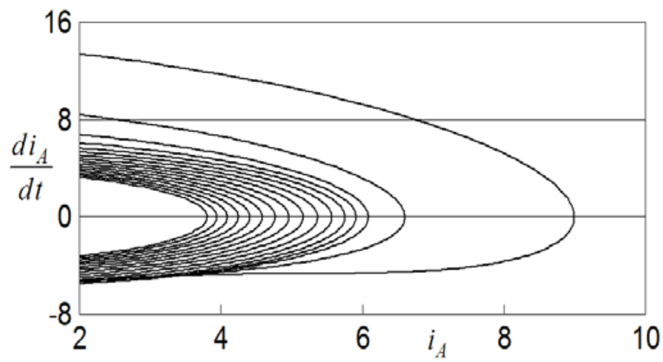

Figure 6(b): Diagram encompassing the stator phase current relative maxima

Figure 6: Pair of diagrams encompassing the relative minima and the relative maxima of stator phase current (14), respectively, for $\gamma_0 = -\pi/2$ in (17)

By extending the criterion of data recording advanced in [5], and used there to localize the relative extrema of characteristic quantities by highlighting small areas of interest encompassing the stationary points and the critical values, one perceives the possibility of detecting the critical values by limiting enough the domain of characteristic quantities derivatives that is, in our case, the ordinates interval. We recall here that, in our case, the characteristic quantity is the stator phase *A* current (14), which has the time-related derivative yielded by (19). In this context, in contrast to the curves plotted in Figure 3 up to Figure 6, the segments plotted in Figure 7 up to Figure 10 have been obtained by computing and recording the value of stator phase current only if the absolute value of stator phase current derivative (19) has been found less than value $\varepsilon = 0.25$. Thus, having in view the adopted coordinate system, the stator phase current (14) has been evaluated and recorded only if the condition

$$\left| \frac{di_A}{dt} \right| < \varepsilon$$

$$\Leftrightarrow \left| \left(\frac{di_d}{dt} - \omega_r \, i_q \right) \cos\gamma + \left(\frac{di_q}{dt} + \omega_r \, i_d \right) \sin\gamma \right| < \varepsilon; \quad \varepsilon = 0.25 \tag{20}$$

has been met.

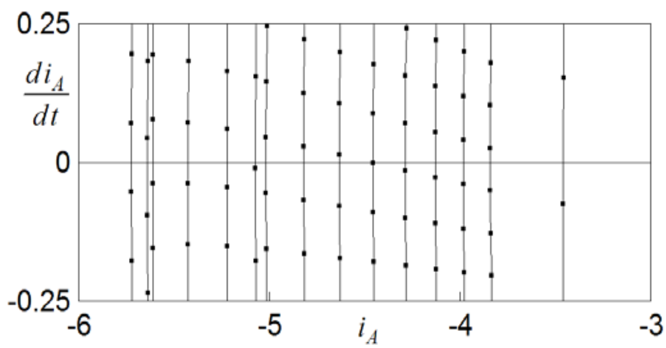

Figure 7(a): Diagram corresponding to stator phase current relative minima

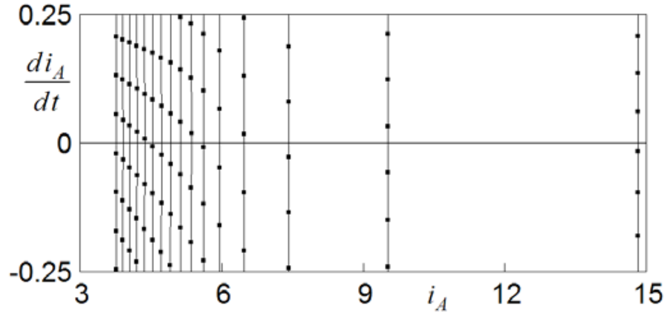

Figure 7(b): Diagram corresponding to stator phase current relative maxima

Figure 7: Diagrams corresponding to stator phase current relative minima and relative maxima, respectively, for the circumstance of $\gamma_0 = 0$ in (17)

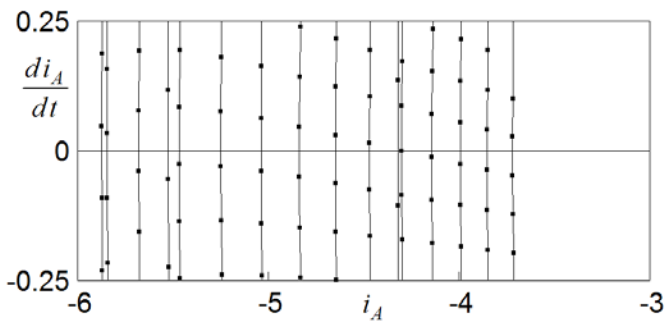

Figure 8(a): Diagram corresponding to stator phase current relative minima

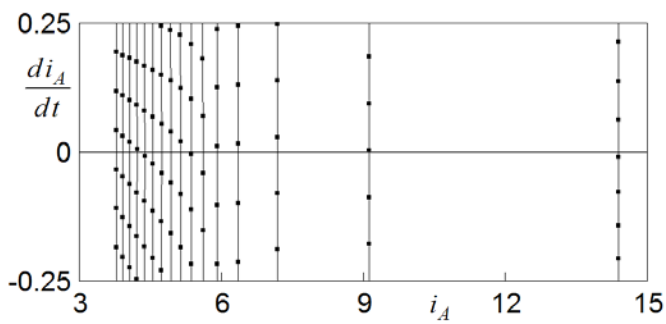

Figure 8(b): Diagram corresponding to stator phase current relative maxima

Figure 8: Diagrams corresponding to stator phase current relative minima and relative maxima, respectively, for the circumstance of $\gamma_0 = -\pi/6$ in (17)

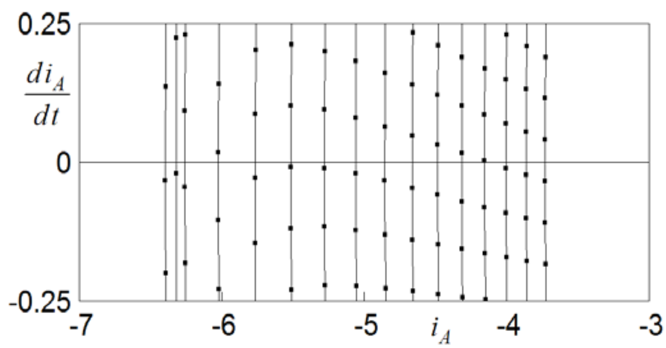

Figure 9(a): Diagram corresponding to stator phase current relative minima

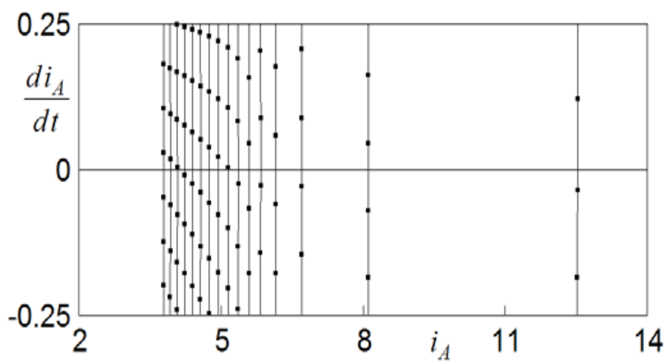

Figure 9(b): Diagram corresponding to stator phase current relative maxima

Figure 9: Diagrams corresponding to stator phase current relative minima and relative maxima, respectively, for the circumstance of $\gamma_0 = -\pi/3$ in (17)

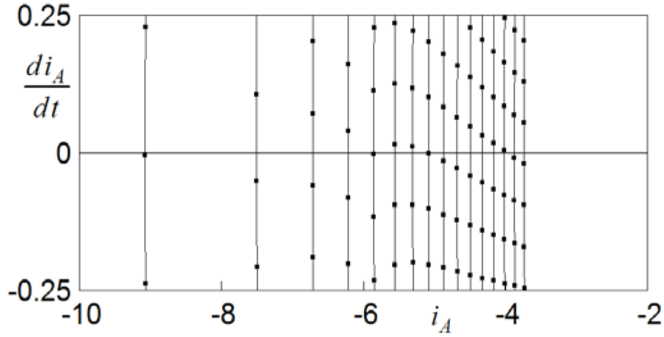

Figure 10(a): Diagram corresponding to stator phase current relative minima

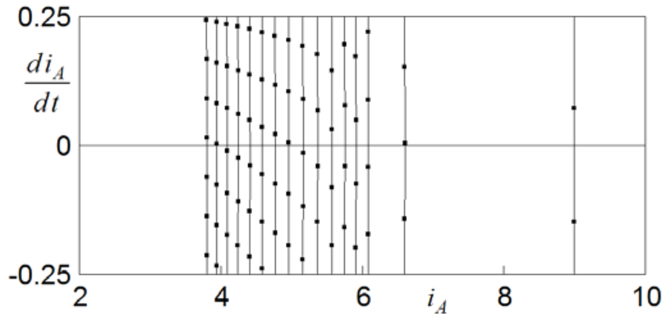

Figure 10(b): Diagram corresponding to stator phase current relative maxima

Figure 10: Diagrams corresponding to stator phase current relative minima and relative maxima, respectively, for the circumstance of $\gamma_0 = -\pi/2$ in (17)

It has to be emphasized that since the ordinate of the introduced coordinate system is represented by the characteristic quantity derivative, the recording of the time-related derivative of the selected characteristic quantity is to be performed only over the restricted interval. Thus, in our case, the stator phase current derivative (19) has been evaluated at each step of numerical integration but it has been recorded only if its value has been detected within the adopted interval

$(-\varepsilon, \varepsilon) \equiv (-0.25, 0.25)$.

To receive the plots advanced in this paper, we have employed Lazarus RAD/IDE [14, 15] on Ubuntu Desktop OS.

Since the segments in Figure 7 up to Figure 10 approach to line segments, all the abscissae of the recorded data points that form these segments represent approximations for the critical values (minima and maxima, respectively) of the characteristic quantity.

4 Conclusion

Starting from the observation [1] that the traditional approach to evaluation of the transient scenarios in electrical systems i.e. by generating huge files that contain the data received at all steps during numerical integration, followed by plotting the numerical results over the entire selected time interval is very time consuming and inappropriate from the practical point of view, the present investigation advances a visualization technique for detecting the critical values of the characteristic quantities that describe an electrical transient episode. The proposed technique requires the employment of a Cartesian coordinate system with the abscissa representing a certain characteristic quantity value and the ordinate designating the corresponding time-related derivative of the characteristic quantity. Such kind of coordinate system is usually employed just to evaluate the dynamic stability of an electrical system described by a single autonomous ordinary differential equation.

For the more intricate scenario of sudden three-phase short circuit fault at the terminals of a salient-pole synchronous generator and for various circumstances, we have shown that an adequate limitation of the interval of the characteristic quantity time-related derivative enables both the detection of the characteristic quantity critical values and the significant reduction of the size of files containing the data recorded during numerical integration.

Although it requires software development, we consider that the proposed visualization technique can straightforwardly be implemented within the available environments or it can plainly be employed as a stand-alone solution whenever the online evaluation is essential.

References

[1] W.H. Enright, Software for ordinary and delay differential equations: Accurate discrete approximate solutions are not enough, *Applied Numerical Mathematics*, **56**(3-4), (2006), 459-471.

[2] J. Mahseredjian, S. Dennetiere, L. Dube, B. Khodabakhchian and L. Gerin-Lajoie, On a new approach for the simulation of transients in power systems, *Electric Power Systems Research*, **77**(11), (2007), 1514-1520.

[3] N. Watson and J. Arrillaga, *Power Systems Electromagnetic Transients Simulation*, The Institution of Electrical Engineers (IEE), London, UK, 2003.

[4] J.R. Marti and L.R. Linares, Real-time EMTP-based transients simulation, *IEEE Transactions on Power Systems*, **9**(3), (1994), 1309-1317.

[5] L. Lupsa-Tataru, Procedure of assessing the electrical transients with a view to relative extrema localization, *Journal of Computations & Modelling*, **3**(4), (2013), 263-285.

[6] L. Bessonov, *Applied Electricity for Engineers*, MIR Publishers, Moscow, Russia, 1968, (586-588: "Phase plane analysis").

[7] I. Boldea, *The Electric Generators Handbook: Synchronous Generators*, CRC Press, Boca Raton, FL, USA, 2006, (Ch. 5: "Synchronous generators: Modeling for transients").

[8] A.A. Gorev, *Transient Processes of Synchronous Machine*, Nauka, Sankt-Petersburg, Russia, 1985.

[9] L. Lupsa-Tataru, An extension of flux linkage state-space model of synchronous generators with a view to dynamic simulation, *WSEAS Transactions on Power Systems*, **1**(12), (2006), 2017-2022.

[10] F. Castelli-Dezza, A. Silvestri and D. Zaninelli, The IEC 909 standard and dynamic simulation of short-circuit currents, *European Transactions on Electrical Power Engineering*, **4**(3), (1994), 213-221.

[11] O.E. Roennspiess and A.E. Efthymiadis, A comparison of static and dynamic short circuit analysis procedures, *IEEE Transactions on Industry Applications*, **26**(3), (1990), 463-475.

[12] J.C. Butcher, Numerical methods for ordinary differential equations in the 20th century, *Journal of Computational and Applied Mathematics*, **125**(1-2), (2000), 1-29.

[13] T.E. Hull, W.H. Enright, B.M. Fellen and A.E. Sedgwick, Comparing numerical methods for ordinary differential equations, *SIAM Journal on Numerical Analysis*, **9**(4), (1972), 603-637.

[14] M. Van Canneyt, *Programmer's Guide for Free Pascal, Version 2.6.0*, Document version 2.6, December 2011, www.freepascal.org

[15] M. Van Canneyt, M. Gärtner, S. Heinig, F. Monteiro de Cavalho and I. Ouedraogo, *Lazarus. The Complete Guide*, ProPascal Foundation, www.blaisepascal.eu, www.lazarus.freepascal.org